



# Influence of confinement on conformational entropy of a polymer chain and structure of polymer–nanoparticles complexes

Waldemar Nowicki<sup>a,\*</sup>, Grażyna Nowicka<sup>a</sup>, Jolanta Narkiewicz-Michałek<sup>b</sup>

<sup>a</sup> Faculty of Chemistry, Adam Mickiewicz University, Grunwaldzka 6, 60-780 Poznań, Poland

<sup>b</sup> Faculty of Chemistry, Maria Curie-Skłodowska University, M. Skłodowska-Curie Pl. 3, 20-031 Lublin, Poland

## ARTICLE INFO

### Article history:

Received 7 January 2009  
Received in revised form  
23 February 2009  
Accepted 26 February 2009  
Available online 11 March 2009

### Keywords:

Self-avoiding walk  
Excluded volume  
Surface curvature

## ABSTRACT

Behaviour of a polymer chain in the presence of fixed obstacles has been studied by the static Monte Carlo simulations. A modified self-avoiding walk on a cubic lattice has been used to model the polymer in an athermal solution. The statistical counting method has been applied to calculate the conformational entropy of the chain, assumed to be grafted to an obstacle. Different chain lengths and obstacle curvatures have been examined. Some implications of the confinement induced changes in the conformational entropy of polymer chains to the structure of complexes composed of long polymer chains and nanoparticles are discussed.

© 2009 Elsevier Ltd. All rights reserved.

## 1. Introduction

Properties of polymer molecules in the vicinity of interfaces are modified by the confinement effect. The thermodynamics of an isolated macromolecule in confining environment is a subject of continuing theoretical interest because of its importance in many areas including biology, medicine and nanotechnology. Predictions of thermodynamic properties of a linear polymer molecule in the presence of a confining environment of particular geometry are of relevance in studying the encapsulation of macromolecules by lipid membranes to form protocellular structures under prebiotic conditions [1–4], the deformation of an elastic film (a bacteria cell membrane) by a chain attached [5], the application of a macromolecule as a localized pressure microtool [6], the interaction between particles coated by end-grafted homopolymers [7], the polymer distribution in joint spherical domains (single or double sphere occupancy) [8], the translocation of a polymer chain through a hole and its biological consequences like the introduction of viral DNA to the cytoplasm of bacterial cell or the exchange of a genetic material in the conjugation of bacteria [9–11], micromanipulation of individual polymer molecules using AFM [12], and many other processes.

The geometrical constraints applied to a free unperturbed polymer chain (like the segment attachment to the surface of an

object or imposition of volume constraints) reduce the number of available conformations of the chain and introduce additional interactions between polymer segments and the surface [13]. Hence, the properties of a polymer chain placed into a confining environment are quite different from those of the chain in the bulk. An essential thermodynamic property of the macromolecule and its environment, which is a measure of the potential energy and the spatial configuration, is the Helmholtz free energy [14]. The thermodynamic generalised forces, such as the pressure gradient, as well as mechanical forces that may exist in the system can be derived from the excess free energy.

There are two contributions to the Helmholtz energy, controlled by the energetic and entropic properties of the system. Although the energy contribution to the free energy can be quite easily found in various simulation approaches, the estimation of the conformational entropy of the chain is a more difficult task. Some attempts aiming at a quantitative calculation of the conformational entropy of polymer chain have been made by Monte Carlo (MC) simulations employing the random self-avoiding walk (SAW) on a lattice. The conformational entropy of a chain with both the excluded volume effect and finite intersegment attractive or repulsive interactions, was estimated by means of the SAW [15] and some modifications of the SAW (e.g. the self-attracting SAW) [15,16]. The exact entropies of free macromolecules were calculated by means of the exact enumeration (EE) method for extremely short chains [17,18] and from an asymptotic analytical equation derived by means of the renormalization group (RG) theory for long chains [19,20]. The conformational entropies of chains of

\* Corresponding author.

E-mail address: [gwnow@amu.edu.pl](mailto:gwnow@amu.edu.pl) (W. Nowicki).

intermediate lengths were obtained by MC simulations associated with the scanning method developed by Meirovitch [21,22], hypothetical scanning method (used also in conjunction with molecular dynamic simulations) [23] or statistical counting (SC) method worked out by Zhao et al. [24]. The latter method was applied to a free unperturbed chain [24] and to a chain terminally attached to an impenetrable surface [25,26] and its results were verified by a comparison with those of EE method and RG theory.

Depending on the polymer concentration, the chains terminally attached to the surface may form structures from “cigars”, built of linear chains of blobs stretched out along the direction perpendicular to the surface, at high polymer concentrations [27] to a “mushroom” structure in low concentration regime, where the mean separation between adjacent macromolecules is large compared to their linear size [27,28]. Some rough approximations of the reduction of the conformational entropy, caused by the “mushroom” structure formation at the flat surface, have been made by Binder [29], who estimated the entropy loss by the expression:  $(\gamma_{\text{free}} - \gamma_{\text{att}})\ln(N)$  with  $\gamma_{\text{free}} - \gamma_{\text{att}} = 0.5$ , where  $N$  is the number of segments in the polymer chain and  $\gamma_{\text{free}}$  and  $\gamma_{\text{att}}$  denote critical exponents referring to the infinite and semi-infinite space, respectively. A similar dependence was proposed by Wu et al. [25] on the basis of estimation of the efficient coordination number, made by Whittington [30]. However, the simulations performed by Wu et al. provided an evidently lower difference in the critical exponents than that obtained by Binder. The situation gets even more complicated if the surface is curved. The terminal attachment of the polymer thread to the apex of the cone causes the conformational entropy reduction with the “universal” exponent  $\gamma_{\text{att}}$  dependent on the conic tip’s angle [31]. Similar behaviour has been found for the entropy of the chain tethered to the planar wedge, both in two- and three-dimensional spaces [32–35].

The volume constraints of macromolecule environment also reduce the number of accessible conformations of polymer chain and, as a result, its conformational entropy. In the case of chains confined in slits [36,37] and within tubes [38], the dependence between the entropy loss and the ratio between an available space and a linear dimension of free polymer coil can be described by a simple power law with the universal exponent  $1/\nu$  (where  $\nu$  is equal to 1/2 and 0.588 for the ideal chain and the SAW model, respectively). The relation between the entropy reduction due to the spherical confinement and the chain length is more complex and the screening of the excluded volume interactions is observed [39].

The macromolecule in an athermal solution can be well modelled by the SAW method on a simple cubic lattice. Nevertheless, some lattice modifications have been used recently in the simulations of proteins and polypeptides. The modifications consisted in the adaptation of different ways of selection of successive repeat units in the chain, i.e. in using different vectors representing the bonds between the nearest neighbour segments, given by permutations of particular coordination sets. For example, Sikorski and Romiszowski [40–43] used a (310) lattice based on the  $(\pm 3, \pm 1, 0)$  coordination set. The polymer chain modelled by this method is very flexible as compared with that generated in a simple cubic lattice. The coordination number of the lattice,  $\omega$ , is very high and equals to 90 (for a simple cubic lattice  $\omega = 6$ ). Moreover, the angles between bonds reproduce conformations of real peptides and proteins with great accuracy. The (311) lattice of  $\omega = 24$  was applied for the simulation of folded protein structure with a lattice chain growth algorithm [44].

The main aim of the work presented here was to study a system composed of a single isolated polymer thread and an obstacle, in terms of its basic thermodynamic properties. In particular, we focused on the study of excluded volume effects using the static MC

method applied to the SAW model. The algorithm of selection of the segment location employed, based on (112) lattice representation, is efficient for high segment densities and impenetrable interfaces examined in this study. As the results obtained for the SAW model can be related to the properties of a macromolecule in the athermal solution, we studied the conformational entropy as the crucial quantity fully determining the system properties. Although the paper discusses only simplified athermal model of the polymer solution, our results can be also used in the analysis of the entropy contribution in the free energy of more complicated systems, governed by specific interactions (e.g. electrostatic potentials necessary for the full description of systems containing biopolymers).

We have calculated the entropy and the free energy of deformation of a polymer coil caused by its irreversible attachment with one segment to surfaces of different curvatures. The conformational entropies obtained were used in the analysis of the structure of objects built of a long polymer thread and nanoparticles.

## 2. Model

### 2.1. Generation of a polymer chain

We generated a sequence of statistically independent samples of chain conformation by means of the static Rosenbluth–Rosenbluth MC approach [45,46]. Each simulation was performed in the three-dimensional primitive regular cubic lattice of a lattice constant  $a$ . The simulation box contained one linear chain and, in some simulations, obstacles of flat or curved surfaces. The chain was represented by the modified SAW. The modification concerns the way of the segment positioning in the lattice. Instead of the standard SAW model exhaustively described in Refs. [45–47], in which each segment links two nearest lattice nodes, we used the algorithm, in which the segments of the chain were connected by vectors of the type  $[\pm a, \pm a, \pm 2a]$ ,  $[\pm a, \pm 2a, \pm a]$  and  $[\pm 2a, \pm a, \pm a]$ . Further in the text, this algorithm is referred to as the (112) motion. A fragment of the chain generated by this algorithm is shown in Fig. 1. This generation method is similar to those applied for

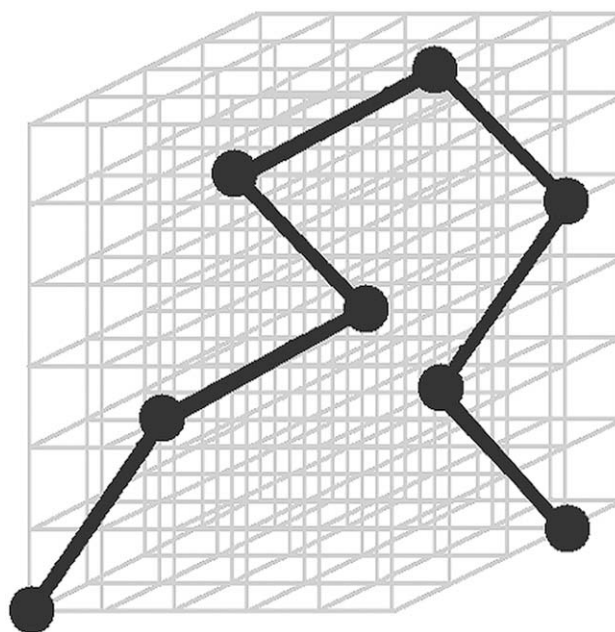


Fig. 1. Visualization of the (112) SAW on a 3D cubic lattice. Circles denote lattice sites blocked by segments connected by bonds generated by means of (112) algorithm.

simulations of polypeptides, where (123) and (023) algorithms were used [43,44], and gives the coordination number  $\omega$  equal to 24. Such a high value of  $\omega$  results in a very large flexibility of the chains generated.

No interactions are considered in the model except the excluded volume of the polymer chains and the obstacles, i.e. no long range and local potentials are present. In consequence, the system behaves similarly to the athermal one and hence our model gives an estimation of good solvent conditions [48].

The segment length  $l$  was equal to  $\sqrt{6}a$ . The volume of the simulation box was equal to  $(601a)^3$ . The periodic boundaries of the space were adopted. Simulations were performed for free (unperturbed) chains and for those attached with one segment to the surface of an obstacle. Obstacles of flat and curved surfaces were applied by blocking appropriate lattice sites prior to the chain generation. The surface of obstacles was rigid and impenetrable to the polymer. The surface was purely repulsive and there was no chain adsorption (athermal surface) except the irreversible attachment of an arbitrarily chosen segment. In consequence, the influence of the surface on the polymer conformation was solely of entropic character. The sites occupied by the obstacle and by the polymer were marked in different ways in the space array. This permitted distinction between the excluded volume effects caused by the obstacle and by the chain. In order to simulate the conformation of the macromolecule attached to the surface not by a terminal segment but by another arbitrarily chosen one, two SAW chains starting at the same point were generated. The sum of the segment numbers in both chains was equal to the segment number in the whole chain.

The chains of up to 1000 segments were considered. Each segment occupied one lattice site. The number of sites blocked by the obstacle was determined by the shape and the size of the obstacle – all network sites placed at the distance larger than the curvature radius of concave obstacles (cavities) or inside convex obstacles (particles) were blocked. The position of the obstacle in the simulation box was chosen in such a way that the macromolecule generated was located in the central part of the simulation box.

Each data set presented in the paper was calculated as an average of results obtained from  $10^5$  chain conformations. The entropy results calculated by means of SC method converge fast to the average; the relative standard deviation for the chain of 1000 segments obtained by 50 independent data sets of  $10^5$  conformations was equal to  $3.3 \times 10^{-6}$ .

## 2.2. Calculation of conformational entropy of a chain

The conformational entropy of the SAW chain was calculated by means of the SC method [24]. The method is based on the calculation of the quantity defined as:

$$\omega'_{\text{eff}}(i) = \frac{Q(i+1)}{Q(i)} \quad (1)$$

where  $Q(i)$  is the number of conformations of the chain of  $i$  segments. The physical meaning of  $\omega'_{\text{eff}}$  can be related to the effective coordination number of the lattice. For the (112) algorithm on the cubic lattice it takes a value of 24 for the first segment, then  $\omega'_{\text{eff}} \leq 23$ . If  $\omega'_{\text{eff}}$  values are known, the total number of conformations of a chain built of  $N$  segments can be calculated from the equation:

$$Q(N) = \prod_{i=1}^{N-1} \omega'_{\text{eff}}(i) \quad (2)$$

In our study, instead of  $\omega'_{\text{eff}}$ , the average values obtained by the MC sampling method,  $\omega_{\text{eff}}$ , were used. The entropy of the chain,  $S$ , was calculated from the equation:

$$\frac{S}{k_B} = \sum_{i=1}^{N-1} \ln(\omega_{\text{eff}}(i)) \quad (3)$$

where  $k_B$  is the Boltzmann constant.

In practice, the effective coordination number,  $\omega_{\text{eff}}$ , corresponds to the number of all empty sites (sites not filled by other segments or by an obstacle) available for the placement of a successive segment at each generation step. Finally, following Eq. (3), the conformational entropy of the single chain was calculated as a sum of logarithms of effective coordination numbers equivalent to empty lattice sites found at each step of the chain generation. In addition to the counting of empty sites, the sites occupied by the obstacle and by the chain were also counted, in order to estimate the excluded volume effects of the obstacle and the chain separately.

In order to verify whether the method applied gives acceptable results, the dependencies of the conformational entropy vs. the segment number obtained for the unperturbed polymer chain were carefully checked by comparison with the equation derived by RG theory (see Section 3.1).

## 3. Results

### 3.1. Free chain and chain terminally attached to a flat surface

As has been proved by a comparison with the EE method and the RG theory, the SC method gives correct results of the conformational entropy of free (001) SAW chains [24,26]. We employed the method for the calculation of the effective coordination number and the conformational entropy for (112) SAW in the system studied here. In order to check the validity of the assumptions of the model, we performed our calculation at first for the free chain. The results of the calculation are shown in Figs. 2 and 3a. As seen in Fig. 3a, the  $\omega_{\text{eff}}$  starts with the value equal to the maximum coordination number (24) of the lattice and then asymptotically

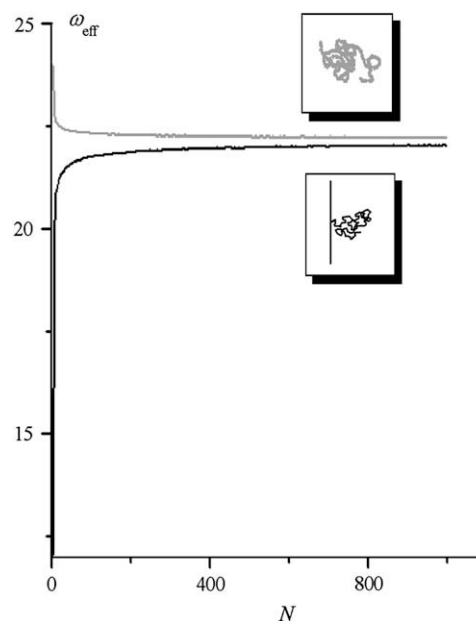
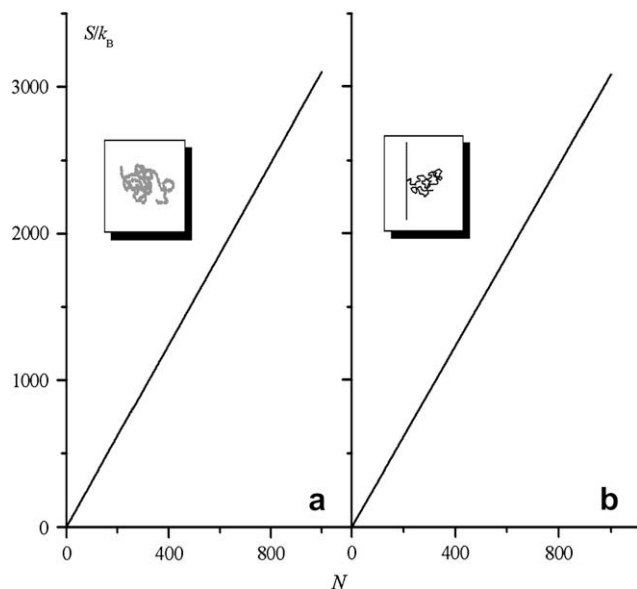


Fig. 2. The effective coordination number  $\omega_{\text{eff}}$  vs. the chain length  $N$  (grey line – a free chain, black line – a chain terminally attached to a flat surface).



**Fig. 3.** The dependence of the chain conformational entropy  $S$  on the chain length  $N$ : (a) a free chain, (b) a chain terminally attached to a flat surface.

decreases to a value approximately of 22.22. The conformational entropy vs. the chain length relation exhibits almost a linear trend as illustrated in Fig. 3a. Numerical analysis of the simulation results revealed that this relationship can be well described by the formula derived from the RG theory for  $N \rightarrow \infty$  [19,20]:

$$\frac{S}{k_B} = \ln(C_{\text{free}}) + (\gamma_{\text{free}} - 1)\ln(N) + N \ln(\omega_{\text{eff,free}}) \quad (4)$$

where a constant  $C_{\text{free}}$  and an effective coordination number  $\omega_{\text{eff,free}}$  are the parameters dependent on the microscopical details of the network applied and  $\gamma_{\text{free}}$  is the universal exponent.

Table 1 presents the results of the fit of parameters of Eq. (4) to the simulation results calculated by means of the nonlinear Levenberg–Marquardt least square method [50]. Since the  $S = f(N)$  dependence is almost exactly linear, the fitting was performed with some parameters fixed. As seen, the parameters dependent on the geometry of the lattice ( $C_{\text{free}}$ ,  $\omega_{\text{free}}$ ) take different values for the (001) and (112) models. The effective coordination number obtained for (112) SAW agrees with the result obtained by the direct estimation of  $\omega_{\text{eff}}$  from data collected in Fig. 2. The universal exponent  $\gamma_{\text{free}}$  is close to the value 7/6 predicted by RG theory [51], which indicates that the algorithms and methods of computation of the conformational entropy of the free chain applied in the present work give satisfactory results.

When a chain is terminally attached to an impenetrable planar surface, half of the lattice sites in the nearest neighbourhood of the segment anchored is filled by the obstacle. Hence, the effective

**Table 1**

Comparison of the parameters of Eq. (4) for (001) and (112) SAW chains, taken from the literature and obtained by the fitting procedure, respectively.

Model	$C_{\text{free}}$	$\gamma_{\text{free}}$	$\omega_{\text{eff,free}}$
(001)	1.17 [49]	1.17 [50]	4.6838 [50]
(112)	$1.160 \pm 0.004$	$1.17^a$	$22.22^a$
	$1.291 \pm 0.009$	$1.17^a$	$22.2151 \pm 0.0003$
	$1.23 \pm 0.03$	$1.157 \pm 0.004$	$22.22^a$
	$0.525 \pm 0.009$	$1.363 \pm 0.004$	$22.2021 \pm 0.0003$

<sup>a</sup> Fixed parameters.

coordination number starts at 12 and then tends asymptotically to a value close to that obtained for the free chain (see Fig. 2). The absolute values of the conformational entropies of the unperturbed chains and of the chains tethered to an inert, impenetrable flat surface do not differ significantly from each other, as illustrated in Fig. 3.

The attachment of the terminal segment to the surface involves several effects which can influence both the energy and the entropy of the system. Generally, at a constant temperature, the free energy of the chain attachment to the obstacle surface,  $\Delta A$ , can be expressed as:

$$\frac{\Delta A(N)}{k_B T} = \frac{\Delta U}{k_B T} - \frac{\Delta S(N)}{k_B} = \text{const} - \frac{\Delta S(N)}{k_B} \quad (5)$$

where  $\Delta U$  is the energy of irreversible attachment of the chain segment to the surface and  $\Delta S(N)$  denotes the change in the conformational entropy caused by both the transfer of the chain of length  $N$  from the bulk to near the surface and the attachment of its terminal segment to this surface. According to athermal assumptions made above, the free energy vs. chain length dependence can be expressed solely in terms of the change in the chain conformational entropy  $\Delta S$ .

The difference between the conformational entropy of free ( $S_{\text{free}}$ ) and attached ( $S_{\text{att}}$ ) chains, further referred to as the chain attachment entropy ( $\Delta S \equiv S_{\text{att}} - S_{\text{free}}$ ), calculated for different chain lengths, is shown in Fig. 4. Whittington [30] and Wu et al. [25] postulated that the conformational entropy of the chain terminally attached to the flat impenetrable surface can be described by the expression similar to Eq. (4):

$$\frac{S}{k_B} = \ln(C_{\text{att}}) + (\gamma_{\text{att}} - 1)\ln(N) + N \ln(\omega_{\text{eff,att}}) \quad (6)$$

where  $C_{\text{att}}$ ,  $\omega_{\text{eff,att}}$  and  $\gamma_{\text{att}}$  are the parameters characterizing the attached chain. Consequently, the chain attachment entropy,  $\Delta S$ , can be calculated as the difference between the values defined by Eqs. (6) and (4):

$$\frac{\Delta S}{k_B} = \ln \frac{C_{\text{att}}}{C_{\text{free}}} + \beta \ln N + N \ln \frac{\omega_{\text{eff,att}}}{\omega_{\text{eff,free}}} \quad (7)$$

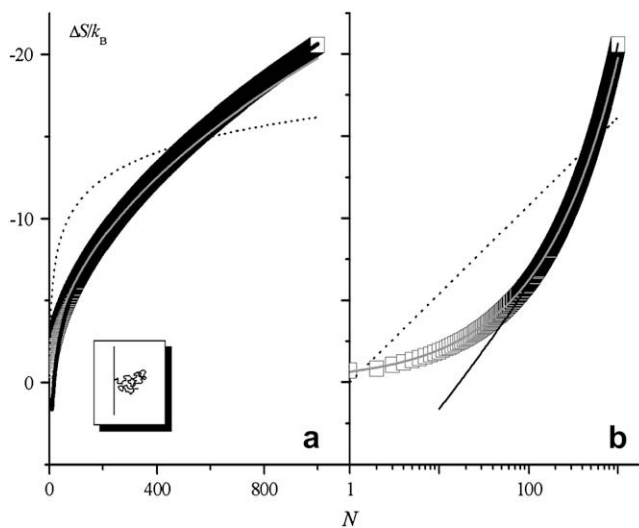


**Fig. 4.** The entropy of the terminal attachment of a chain to a flat surface: (a) the double linear dependence, (b) the linear-logarithmic dependence (the black line – results calculated from Eq. (7), the dotted line – results of Eq. (8), the grey line – results calculated from Eq. (9), squares – results of the simulation).

Whittington [30] and Wu et al. [25] proposed a simplification of Eq. (7). The simplification is based on the assumption that for very long chains  $C_{\text{free}} \approx C_{\text{att}}$  and  $\omega_{\text{eff,free}} \approx \omega_{\text{eff,att}}$ , so that the logarithms of the corresponding ratios are close to zero and, hence, one obtains:

$$\frac{\Delta S}{k_B} = (\gamma_{\text{att}} - \gamma_{\text{free}}) \ln N = \beta \ln N \quad (8)$$

As seen in Fig. 4, Eq. (8), as well as a more general Eq. (7), poorly fits the simulation results. Eq. (7) gives satisfactory results only for large chain lengths ( $N > 500$ ); for shorter chains the fit is poor. The analysis of the  $\ln(\Delta S) = f(\ln(N))$  dependence shows that this relationship can be expressed by a simple power law:

$$\frac{\Delta S}{k_B} = -H_1 N^{b_1} \approx -H_1 \sqrt{N} \quad (9)$$

where  $H_1$  and  $b_1$  are constants.

For short chains, the best fit to the simulation results is produced by Eq. (9) (Fig. 4). The numerical values of the fitted parameters of Eqs. (7)–(9) are listed in Table 2.

The scaling law reported by Eq. (9) is a consequence of the reduction of the chain conformation number  $\Delta Q$  caused by the cut-off of only peripheral parts of the polymer coil by the planar surface [26]. Since the reduction of the conformational entropy is relatively low it is proportional to the reduction of conformation number since

$$\Delta S \sim \ln\left(\frac{Q_{\text{att}}}{Q_{\text{free}}}\right) \sim \ln\left(1 - \frac{\Delta Q}{Q_{\text{free}}}\right) \sim -\frac{\Delta Q}{Q_{\text{free}}}.$$

### 3.2. Chain terminally attached to a convex surface

The effective coordination numbers calculated for the chains terminally attached to convex surfaces of different curvature radii,  $R$ , are shown in Fig. 5a. The  $\omega_{\text{eff}}$  vs.  $N$  dependencies lie in between those obtained for the unperturbed chains in the bulk and the chains terminally attached to the flat surface. The smaller the radius, the smaller the difference between the values obtained for the free and surface bound chains, except for the region of  $N \leq 50$ . The objects of very small radii ( $R \leq 3l$ ) practically do not affect the value of the effective coordination number as compared with that of the unperturbed chain. As seen in Fig. 5a, with increasing  $N$ , the values of  $\omega_{\text{eff}}$  asymptotically tend to the value corresponding to the unperturbed chain.

The weak influence of small objects on the conformational entropy of attached chains is also evidenced from the  $\Delta S$  vs.  $N$  dependencies, collected in Fig. 5b. The smaller the object radius, the smaller the excluded volume, and hence the smaller the entropy reduction. For extremely small objects, i.e. those whose radii are comparable with the polymer segment length ( $R \leq 3l$ ), the entropy loss becomes independent of  $N$  (horizontal lines). It means that such small objects bring about only a local perturbation in the coil conformation. Thus, for  $N \rightarrow \infty$  the value of  $\Delta S$  depends only on the object volume [26],  $V_p$ :

**Table 2**

The parameters of Eqs. (7)–(9) obtained by the fitting procedure.

Equation number	Symbol of parameter	Value of parameter
(7)	$C_{\text{free}}/C_{\text{att}}$	$17.6 \pm 1.5$
	$\beta$	$-1.78 \pm 0.02$
	$\omega_{\text{eff,free}}/\omega_{\text{eff,att}}$	$0.9885 \pm 0.0001$
(8)	$\beta$	$-2.34 \pm 0.02$
(9)	$H_1$	$0.650 \pm 0.002$
	$b_1$	$0.500 \pm 0.001$

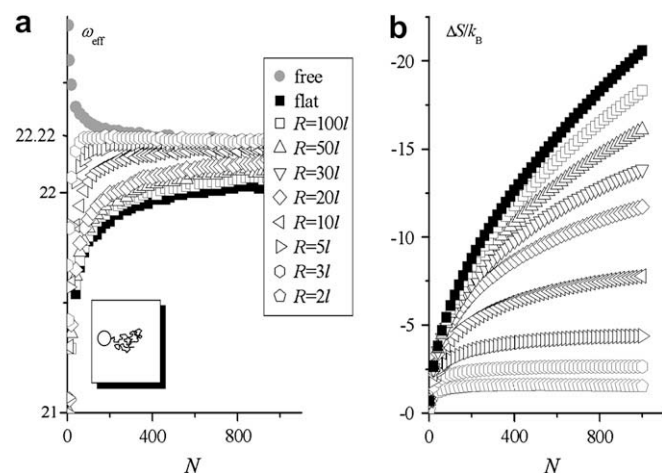


**Fig. 5.** Plots of  $\omega_{\text{eff}}$  vs.  $N$  (a) and  $\Delta S$  vs.  $N$  (b) for the chains terminally attached to convex surfaces of different curvature radii  $R$  (values of  $R$  are marked in figure). The dependence for free chains is also given for comparison.

$$\frac{\Delta S}{k_B} = \frac{1}{2} \ln V_p \quad (10)$$

### 3.3. Chain terminally attached to a concave surface

The generation of a polymer chain which is terminally attached to the inner surface of a sphere is a difficult task in a situation when the sphere volume is small and especially, when the number of the lattice sites in the available space is comparable with the number of polymer segments. The difficulty could be overcome satisfactorily by applying the modified (112) SAW model. The modified algorithm presented produces very a flexible chain which can be quite easily packed into small cavities especially if the algorithm generating the chain chooses each following segment position only from empty lattice sites. The algorithm allowed generation of a chain consisting up to 1000 segments and confined into a spherical cavity with a radius as small as  $5l$  (such a cavity can comprise about 7700 segments). For the cavity radii of  $4l$  and  $3l$  the mean number of segments in the successfully generated chains was 720 and 300, respectively, which correspond to the segment concentration in the cavity of about 0.18. The simulation results are collected in Fig. 6, showing  $\omega_{\text{eff}}$  vs.  $N$  (Fig. 6a) and  $\Delta S$  vs.  $N$  (Fig. 6b) curves obtained for the chains terminally attached to the inner surface of cavities of different radii. As seen, for extremely small cavities (of radii smaller than  $5l$ ) the value of  $\omega_{\text{eff}}$  quickly reduces to zero and the process of chain generation stops. For large cavities, the  $\omega_{\text{eff}} = f(N)$  dependencies are practically linear, except for their initial parts corresponding to very short chains.

One can notice in Fig. 6b that at a certain cavity radius the dependencies between  $\Delta S$  and  $N$  change their bending direction. The  $R$  value at which the reversal of bending direction of curves takes place ( $R = R_c$ ) can be related to the transition between the weak and the strong confinement regimes, introduced by Sakaue and Raphaël [52]. In the  $N$  range examined, the  $R_c$  value does not depend on the chain length but it is influenced by lattice properties. The  $R_c$  value is approximately equal to  $-10l$  (or  $-24.5a$ , see Fig. 6b).

### 3.4. Comparison between different surface curvatures

Fig. 7 presents the  $\Delta S = f(N)$  dependencies in the logarithmic scale, obtained for both concave and convex surfaces. As seen, only

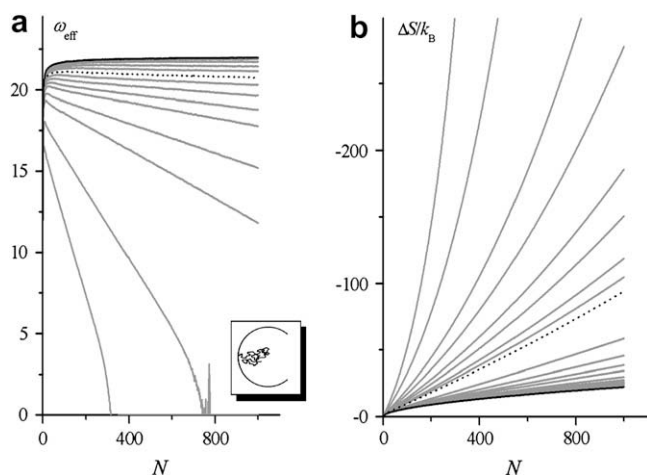


**Fig. 6.** Plots of  $\omega_{\text{eff}}$  vs.  $N$  (a) and  $\Delta S$  vs.  $N$  (b) for the chains terminally attached to concave surfaces of different curvature radii ( $\square - R = -3l$ ,  $\circ - R = -4l$ ,  $\Delta - R = -5l$  and  $\nabla - R = -7l$ ; curves obtained for the flat surface are in black ( $R = \infty$ ); curves at the critical curvature radius ( $R = -10l$ ) are dotted).

the dependence obtained for the flat surface can be approximated by a power law. The relationships obtained for curved surfaces deviate from the power-law behaviour. The smaller the curvature radius of the surface, the greater the deviation. The magnitude of the deviation can be attributed to an increase in the value of the second logarithmic component of Eq. (7) with decreasing  $R$ .

Fig. 8a shows an exemplary dependence of  $\ln(|\Delta S|)$  on the absolute value of  $R$  ( $|R|$  describes surface curvatures of the same magnitude but of the opposite signs) for a chain built of  $N = 1000$  segments. In the range of small values of  $|R|$  the differences in entropies calculated for concave and convex surfaces are

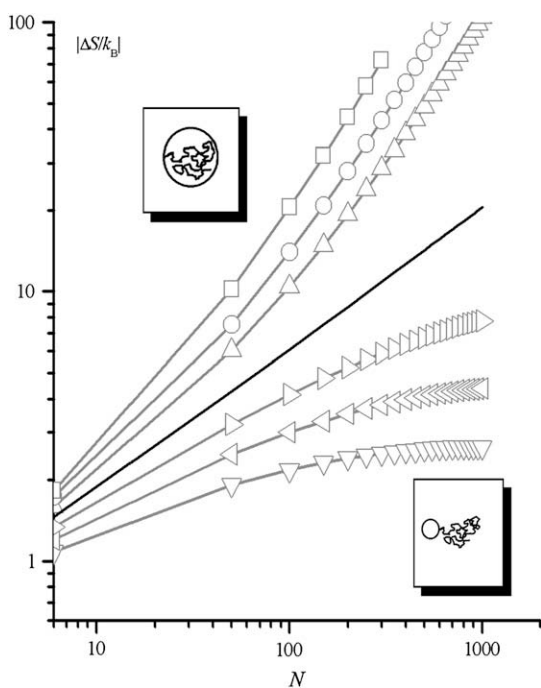


**Fig. 7.** Plots of  $\Delta S$  vs.  $N$  for surfaces of different curvatures ( $\square - R = -3l$ ,  $\circ - R = -4l$ ,  $\Delta - R = -5l$ ,  $\nabla - R = -7l$ ,  $\triangleleft - R = 2l$ ,  $\triangleleft - R = 3l$  and  $\triangleright - R = 4l$ ). The straight line marked in black represents the case of flat surface.

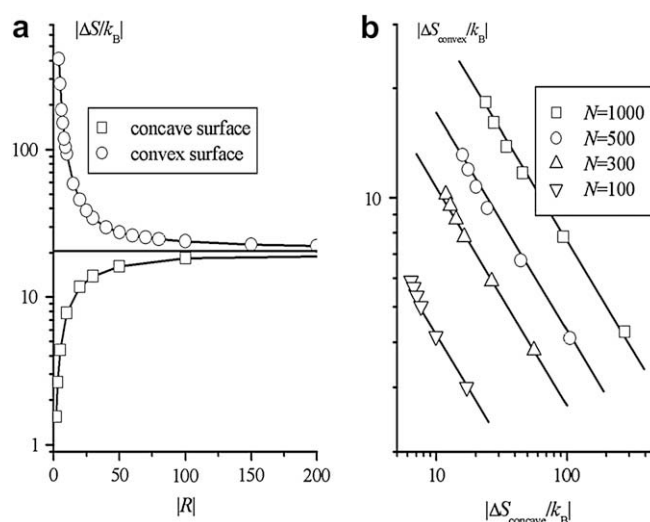


**Fig. 8.** The dependence of  $|\Delta S|$  on the absolute value of the surface curvature radius for  $N = 1000$  (a) and  $\Delta S_{\text{convex}}$  vs.  $\Delta S_{\text{concave}}$  dependencies for different chain lengths (b).

significant, and the smaller the absolute radius, the greater the difference. With the flattening of surfaces the difference vanishes and, in both cases, when  $|R| \rightarrow \infty$  the values of  $\ln(|\Delta S|)$  tend to a common value, corresponding to the entropy of chain attachment to the flat surface.

An interesting feature of the  $\ln(|\Delta S|) = f(|R|)$  plots is that for the same  $N$ , they are almost symmetrical with respect to the ordinate equal to  $\ln(|\Delta S|)$  for the flat surface. This symmetry allows the formulation of an approximate power relation:

$$(\Delta S_{\text{convex}}(R))^{b_2} \Delta S_{\text{concave}}(-R) = (\Delta S_{\text{flat}})^{1+b_2} \quad (11)$$

where  $\Delta S_{\text{convex}}$ ,  $\Delta S_{\text{concave}}$  and  $\Delta S_{\text{flat}}$  denote the entropies of the chain attachment to convex, concave and flat surfaces, respectively. As illustrated in Fig. 8b, the lines calculated from Eq. (11) at  $b_2 = 1.60 \pm 0.01 \approx 8/5$  well reproduce the simulation results.

There are two factors influencing the effective coordination number and, hence, the conformational entropy of the polymer in the vicinity of the surface: the excluded volume of the polymer segments and the excluded volume of the obstacle. In order to handle both factors separately, we have enumerated lattice sites blocked by the polymer segments and by the obstacle. Thus, the effective coordination number can be divided into three components:

$$\omega_{\text{eff}}(i) = \omega - (\alpha_{\text{chain}}(i) + \alpha_{\text{surf}}(i)) \quad (12)$$

where  $\alpha_{\text{chain}}$  and  $\alpha_{\text{surf}}$  are the mean numbers of lattice sites blocked by the polymer segments and the object of a given shape, respectively. The effective coordination number and its components are functions of the segment's number  $i$ .

The results obtained for both concave and convex surfaces are collected in Figs. 9–11.

As seen in Fig. 9, the dependencies between  $\alpha_{\text{surf}}$  and  $N$ , when plotted on a log–log scale, are not straight lines, except for the flat surface. For the chains attached to convex surfaces all dependencies between  $\alpha_{\text{surf}}$  and  $N$  are monotonic in the simulated range of  $N$  values (Fig. 9a). For concave surfaces the  $\alpha_{\text{surf}}-N$  curves have a flat region, whose length increases with a decreasing  $R$  to  $N$  ratio (Fig. 9b). Moreover, for the smallest two cavities of the radii  $R = -4l$  and  $-3l$ , after a certain chain length is exceeded, a sudden increase in  $\alpha_{\text{surf}}$  is observed.

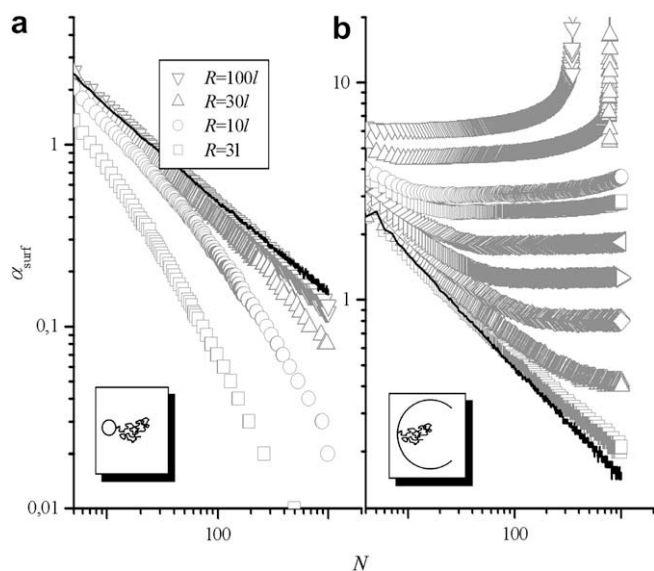


**Fig. 9.** Plots of  $\alpha_{\text{surf}}$  vs.  $N$  for positive (a) and negative (b) values of  $R$  (The straight line marked in black represents the case of  $R = \infty$ , in (b) the cavity radius varies from  $-100l$  to  $-3l$ ).

We found that the plots of  $\ln(\alpha_{\text{surf}}/\alpha_{\text{flat}})$  against  $\ln(N)$ , where  $\alpha_{\text{flat}}$  corresponds to  $R = \infty$ , give straight lines for chains grafted to convex surfaces (Fig. 10). Thus, they can be described by the following approximate expression:

$$\frac{\alpha_{\text{surf}}}{\alpha_{\text{flat}}} = kN^{b_3} + 1 \quad (13)$$

where  $k$  and  $b_3$  are constants;  $b_3 = 0.600 \pm 0.005 \approx 3/5$ .

The properties of the third component of Eq. (12) were also studied in a wide range of chain lengths and surface curvature radii. The results obtained are summarized in Fig. 11 in the form of dependencies between  $\alpha_{\text{chain}}$  and  $N$  for positive (Fig. 11a) and negative (Fig. 11b) values of  $R$ . For convex surfaces (i.e.

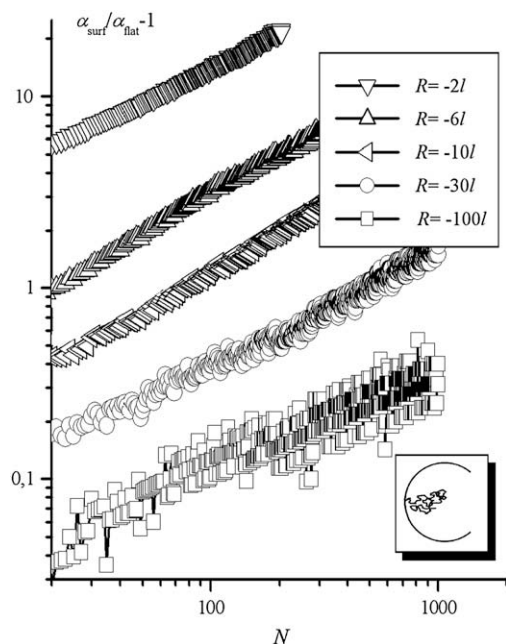


**Fig. 10.** The dependencies  $\alpha_{\text{surf}}/\alpha_{\text{flat}} - 1 = f(N)$  obtained for convex surfaces of different  $R$ .

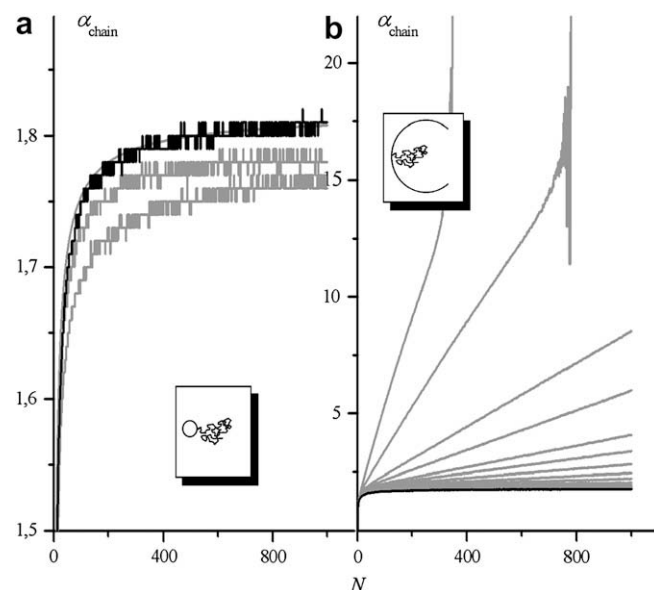


**Fig. 11.** Plots of  $\alpha_{\text{chain}}$  vs.  $N$  for convex (a) and concave (b) surfaces of different curvatures ( $R$  values are equal to  $5l$  and  $30l$  (a) and vary from  $-100l$  to  $-3l$  (b), respectively). The dependence representing the flat surface ( $R = \infty$ ) is also included and marked in black.

spherical objects like, for instance, colloidal particles) the character of the curves is similar in the whole range of  $R$  values. For concave surfaces the shape of the curves changes with the changing  $R$ ; the most distinct changes appear in the range of small values of  $R$ , where a dramatic increase in  $\alpha_{\text{chain}}$  takes place.

The dependencies of the effective coordination number and its components on the segment number shown in Figs. 6a, 9b and 11b are represented by smooth curves which do not exhibit any artificial effects of the lattice properties of the model. Only for relatively long chains and cavity radii equal to  $4l$  or less, the numerical instability caused by the lattice discrete steplike shape of the cavity is observed.

### 3.5. Grafting by any segment

Let's now assume that the segment by means of which a macromolecule is attached to the surface can be located in any position along the chain. Such macromolecule can be represented by two shorter chains terminally attached to the same point of the wall, and consisting of  $N_1$  and  $N_2$  segments. The conformational entropy of this molecule is expected to be smaller than that of the end-attached polymer, because the two parts of the chain mutually restrict the accessible space.

In order to evaluate the contribution of the excluded volume effect, arising from these extra intrachain excluded volume interactions, on the conformational entropy of the whole macromolecule, let us consider a phantom chain, that is a chain divided into two parts by the plane which immobilizes a segment located in the intersection point and is impenetrable to the other segments. In the phantom chain the extra intrachain excluded volume effect is absent, as the two parts of the chain are located at opposite sides of the wall. Thus, the conformational entropy of the phantom chain can be obtained by the summation of the contributions of both its parts. These contributions can be separately calculated from Eq. (9).

In Fig. 12, the influence of the partition ratio  $\zeta$  (which is defined as  $\zeta = N_1/N$ , where  $N_1$  is the number of segments in one of the two parts of the chain) on the conformational entropy of the chain attached is compared to that of the phantom chain. As expected, in the whole range of  $\zeta$  values (except for  $\zeta = 0$  and  $\zeta = 1$ ) the entropy of the attached chain is smaller. The contribution of the extra intrachain excluded volume interactions in the entropy reduction is, as results from the comparison of the corresponding dependencies in Fig. 12, of the same order of magnitude as the contribution arising from the influence of the flat wall on the phantom chain.

The simulation results obtained for the chain attached at any point to the flat surface are well approximated by the equation

$$\frac{\Delta S}{k_B} = -H_1 \sqrt{N} (\sqrt{1-\zeta} + \sqrt{\zeta-1}) \quad (14)$$

with the prefactor equal to  $H_1 = 0.65 \pm 0.01$  as in Eq. (9).

Let us now imagine a process in which the contact point between the polymer and the surface shifts along the chain (the value of  $\zeta$  changes continuously like during the passing a thread through an eye of a needle). Changes in the  $\zeta$  value are accompanied by changes in the conformational entropy of the chain. These, in turn, cause the emergence of the entropic force  $F$ . At a constant temperature this force is equal to the derivative of the change in free energy upon the shift of the chain,  $\Delta A$ , with respect to the length  $x$  of the chain section built of  $N_1$  segments:

$$F = \left(\frac{\partial \Delta A}{\partial x}\right)_T = \left(\frac{\partial \text{const}}{\partial x}\right)_T - T \left(\frac{\partial \Delta S}{\partial x}\right)_T = -T \left(\frac{\partial \Delta S}{\partial x}\right)_T = -\frac{T}{Nl} \left(\frac{\partial \Delta S}{\partial \zeta}\right)_T \quad (15)$$

Finally, the force reads

$$\frac{Fl}{T} = -\frac{1}{N} \left(\frac{\partial S}{\partial \zeta}\right)_T = \frac{H_1 k_B}{2\sqrt{N}} \left(\frac{1}{\sqrt{1-\zeta}} - \frac{1}{\sqrt{\zeta}}\right) \quad (16)$$

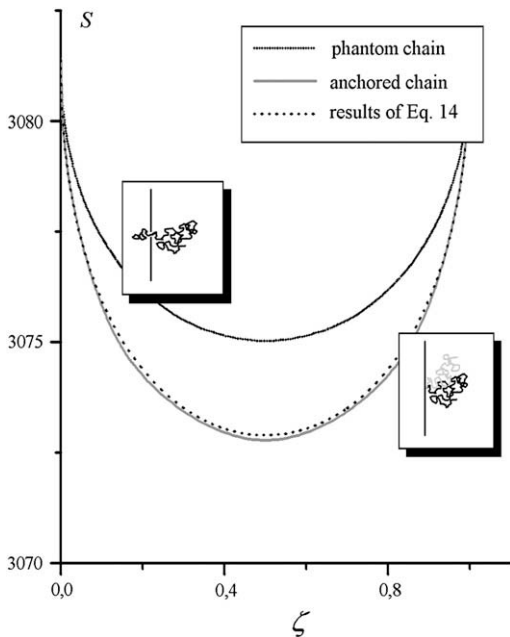


Fig. 12. Conformational entropy of a chain of  $N = 1000$  as a function of the junction point location – comparison of simulation results with those calculated from Eq. (14) and obtained for the phantom chain.

As results from Eq. (16), the net force acting along the chain equals zero for  $\zeta = 1/2$  (which corresponds to the situation when the chain is attached to the surface by its middle segment) whereas the highest absolute value of the force is reached for the terminally attached chain, that is for both  $\zeta = 0$  and  $\zeta = 1$ . Thus, in the light of Eq. (16), one can conclude that if the junction point can move along the chain, the configuration consisting of one long tail is preferable over that of two shorter chains.

Now, let us consider the conformational entropy of a chain which is grafted through an arbitrarily chosen segment to a spherical object (a particle) of the mean curvature radius  $R$ . The effective coordination number of the anchor segment is strongly reduced, which involves changes in  $\omega_{\text{eff}}$  values of the other segments. The extent of change depends on the distance, measured along the chain, from the anchor segment. When the distance increases, the  $\omega_{\text{eff}}$  value also increases tending asymptotically to the common value, approximately equal to 22, as it results from Fig. 13 presenting the dependencies between  $\omega_{\text{eff}}$  and the segment's index  $i$  for different anchor segment locations.

The influence of the partition ratio on the chain conformational entropy for different particle radii is shown in Fig. 14a. All dependencies exhibit minima at the same  $\zeta$  value, corresponding to the attachment through the middle segment. The depth of the minimum increases with the increasing curvature radius of particle, indicating that the larger the object, the greater the entropy loss accompanying the chain attachment (as shown in Fig. 14b).

The relationships between  $S$  and  $\zeta$ , presented in Fig. 16a, can be described by an equation similar to that for the terminal attachment to the flat surface (Eq. (14)), but with the prefactor given by the approximate expression:

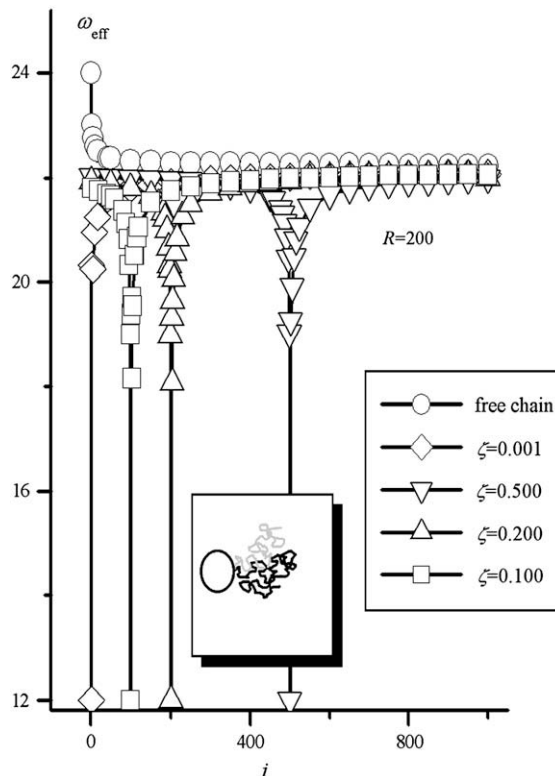
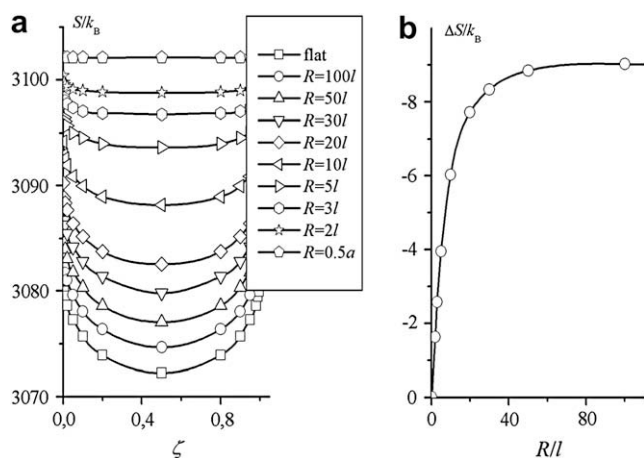


Fig. 13. Dependencies  $\omega_{\text{eff}} = f(i)$  for a chain of  $N = 1000$  and different anchor segment locations (represented by values of  $\zeta$ , which are given in figure).





**Fig. 14.** Relationship between  $S$  and  $\zeta$  for a chain of  $N=1000$  attached to particles of different radii ( $R$  values are indicated in figure) (a) and the depth of minimum (expressed by a difference between  $S$  values corresponding to  $\zeta=0$  and  $\zeta=0.5$  for a given  $R$ ) vs.  $R$  (b).

$$H_2 = \frac{H_1}{1 + B\frac{l}{R}} \quad (17)$$

where the constant  $B = 10.0 \pm 0.05$ .

Now, let us assume as before, that the junction point between the polymer and the particle surface can shift along the chain (the particle can be imagined as a ball rolling along the line). Because the shifting involves changes in the conformational entropy of the chain, the net force  $F$  exerted by the chain on the particle also changes. On the basis of Eq. (14) with prefactor given by Eq. (17) we obtain the following expression for the net force:

$$\frac{Fl}{T} = -\frac{1}{N} \left( \frac{\partial S}{\partial \zeta} \right)_T = \frac{H_1 R k_B}{2(R + Bl) \sqrt{N}} \left( \frac{1}{\sqrt{1-\zeta}} - \frac{1}{\sqrt{\zeta}} \right) \quad (18)$$

The relationships between the separation ratio and the value of  $F$  for different particle radii are shown in Fig. 15. As results, if the polymer is attached by its middle segment, the net force exerted on the particle surface is zero, which is a metastable situation at the entropy minimum. The entropy maximum, which corresponds to the largest force exerted by the chain, is attained when the particle is situated at one of the chain ends. In this situation the system configuration is the most stable.

### 3.6. Complexes with nanoparticles

It is well known that even if the energy of adsorption of a single segment is small, the homopolymer may adsorb quite strongly. It is because a macromolecule attaches to the surface at many contacts and its desorption is highly unlikely, since it requires the rupture of all polymer–surface bonds at the same time [53]. However, if the surface curvature radius is small (as in the case of nanoparticles), the number of polymer–surface contacts is strongly reduced, and thus the polymer detachment can proceed quite readily. It has been shown that if a particle is very small as compared with the size of polymer, the adsorbed chain assumes a conformation with a large fraction of tail segments and only a small fraction in the form of loops with multiple surface contacts [54–57].

Let us now consider a very long homogenous polymer chain (i.e. whose all segments have the same affinity to the surface)

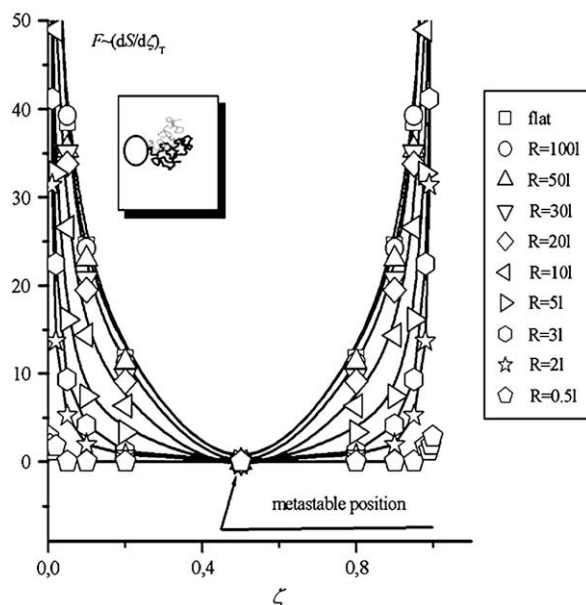


**Fig. 15.** The net entropic force  $F$  exerted by a chain of  $N=1000$  on particles of different radii as a function of the separation ratio  $\zeta$  (values of  $R$  are indicated in figure).

interacting with a small particle ( $R \ll R_G$ ). The initially formed polymer–nanoparticle complex will relax to a state of minimum free energy. The relaxation will proceed through individual segment attachment/detachment events, i.e. when the particle moves along the chain one broken polymer–surface contact is replaced by another newly formed contact, as it is schematically shown in Fig. 16a. If the adsorption energy of individual segments is not too high, the net entropic force originating from the presence of tails will cause the movement of the particle towards one of the chain ends. The particle will not be detached from the chain, if the effect of the increase in internal energy  $\Delta U$  prevails over the effect of the increase in the conformational entropy of the tail, that is if for each desorbing segment the following inequality is fulfilled:

$$\Delta U > T\Delta S \quad (19)$$

Let's notice that  $\Delta U$  of the particle translocation along the chain is equal to zero since each detached segment is replaced by another one. Thus, if the above occurs, one may conclude that the most probable structure of a complex, consisting of a long polymer chain and a nanoparticle, contains one tail only (unlike the two-tail structure postulated elsewhere) [56,57]. This conclusion is consistent with results of Bonet Avalos et al. [55], who found that for rather small adsorption energies a particle has a preference to occupy positions near the edge of the chain.

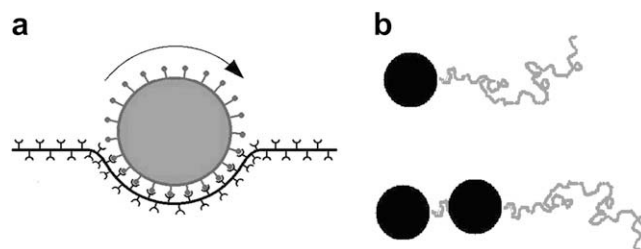


**Fig. 16.** Schematic representation of the movement of a nanoparticle along a polymer chain (a) and the most probable structures of complexes composed of a single polymer chain and reversibly adsorbed nanoparticles (b).



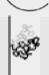
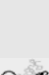
The above considerations can be extended to multiparticle complexes, where two or more particles are attached to a single long polymer chain (Fig. 16b). To this end, let us consider a complex composed of two identical particles whose geometrical sizes as well as the radius of electrostatic repulsion between them are small as compared with the chain length. Assume additionally that before the second particle is being attached, the first one is located at one of the chain ends. The attachment of the second particle can take place somewhere along the chain. Thus, one can distinguish two chain sections in the complex: a tail section with one free end and a bridging section connecting the particles. The shift of the second particle along the chain involves changes in the contributions of both sections to the total entropy of the complex. If the position of the second particle is determined by the partition ratio  $\zeta$ , the entropy change due to the tail formation, as compared with the entropy of the unperturbed chain of the same length, can be assumed to scale as  $(1 - \zeta)^{1/2}$ , according to Eqs. (14) and (17). For the evaluation of the contribution of the bridging section let's suppose that the entropy cost, resulting from the immobilization of two ends of a chain, is equivalent to the entropy reduction caused by the chain confinement into a space of characteristic size  $D$ , which scales with the chain dimension as  $(R_G/D)^2$  [58]. Hence, if one assumes that the timescale of the relaxation of the particle–particle distance is longer than that of the relaxation of the conformation of chain section, the entropy reduction for the bridging section scales as  $\Delta S \sim \zeta^{2\nu}$ . The sum of both contributions gives the asymmetric dependence of the complex entropy vs.  $\zeta$ , which indicates that the situation when both particles are located near the same end of the chain will be preferred.

#### 4. Concluding remarks

The conformation of a linear flexible polymer molecule near impenetrable interfaces of different curvatures has been studied. The study addresses the problem in the athermal limit, in which only excluded volume interactions are considered. The polymer chain was modelled as a self-avoiding walk (SAW) on a cubic lattice. The segment positions in the lattice were chosen by the (112) algorithm. Flat, convex and concave surfaces were considered. The macromolecule was represented by a chain which was either placed in the bulk or permanently attached to the interface through one segment. The effective coordination number of the lattice,  $\omega_{\text{eff}}$ , and the absolute conformational entropy of the chain,  $S$ , were calculated by means of the SC method associated with the static MC sampling method. By introducing the distinction between the lattice sites blocked by the polymer segments and those blocked by an object of a given surface curvature, we were able to estimate relative contributions of the excluded volume effects, arising from intersegmental interactions and from the presence of the interface, in the overall entropy change. On the basis of analysis of simulation results, a power-law correlation between the entropy of the chain terminally attached to the flat wall and the chain length in the range of  $N \in < 1, 1000 >$ , as well as modifications of the correlation for the chains attached to curved interfaces, were formulated. The presented study also revealed that the attachment of the chain through the terminal segment is of the lowest entropy cost as compared with one point attachment by other segments, since in the last case the excluded volume effects of two parts of attached chain interfere. An equation relating the entropy of the chain with its length, the location of an anchor segment and the curvature radius of the interface was formulated. Analysis of the results obtained for convex interfaces allowed some predictions to be made about the structure of complexes composed of long linear macromolecules and nanoparticles.

**Table 3**

Specification of the main processes considered in the paper and the corresponding equations for calculation of changes in conformational entropy of a polymer chain.

System	Process	Equation
	Terminal attachment of a polymer chain to a planar surface	$\Delta S/k_B = -H_1 \sqrt{N}$
	Terminal attachment of a polymer chain to a curved surface	$\Delta S/k_B = -H(R)\sqrt{N} - K(R)N^2$
	Shifting, along a polymer chain, of the location of a segment connecting a macromolecule with a planar surface	$\Delta S/k_B = -H_1 \sqrt{N}(\sqrt{1-\zeta} + \sqrt{\zeta-1})$
	Shifting, along a polymer chain, of the location of a segment connecting a macromolecule with a spherical particle	$\Delta S/k_B = -H_1 \sqrt{N}/(R+B)(\sqrt{1-\zeta} + \sqrt{\zeta-1})$

The precise calculation of the entropy contribution to the excess free energy caused by different spatial constraints of the polymer chains has a relevance that extends well beyond the realm of fundamental polymer physics. The system containing polymer chains tethered to the concave surfaces discussed here can be treated as simplified representation of the DNA molecule tethered inside a protein pore [59] as well as a model of core of polymeric micelles [60]. On the other hand, the polymer chain tethered to the convex surface allows the modelling of the phenomena governing the stability of colloidal systems in the presence of very long polymer chains [61].

In conclusion, the equations for the calculations of changes in the conformational entropy of the polymer chain, caused by the constraints discussed in the paper, are collected in Table 3.

#### Acknowledgment

The work was partially supported by the Scientific Network – Surfactants and Dispersed Systems in Theory and Practice SURUZ (INCO-CT-2003-003355).

#### References

- [1] Deamer DW, Barchweld GL. *J Mol Evol* 1982;18(3):203.
- [2] Srivastava R, Brown JQ, Zhu H, McShane MJ. *Macromol Biosci* 2005;5:717.
- [3] Brown JQ, Srivastava R, McShane MJ. *Biosens Bioelectron* 2005;21(1):212.
- [4] Srivastava R, McShane MJ. *J Microencapsulation* 2005;22(4):397.
- [5] Bickel T, Jeppesen C, Marques CM. *Eur Phys J E* 2001;4:33.
- [6] Bickel T, Marques C, Jeppesen C. *CR Acad Sci Ser IV Phys* 2000;1:661.
- [7] Roan JR, Kawakatsu T. *J Chem Phys* 2002;116:7295.
- [8] Sousa AF, Pais AACC, Linse P. *J Chem Phys* 2005;122:214902.
- [9] Chuang J, Kantor Y, Kardar M. *Phys Rev E* 2002;65:011802.
- [10] Loebel HC, Randel R, Goodwin SP, Mathai CC. *Phys Rev E* 2003;67:041913.
- [11] Tian P, Smith GD. *J Chem Phys* 2003;119(21):11475.
- [12] Bemis JK, Akhremitchev BB, Walker GC. *Langmuir* 1999;15:2799.
- [13] Daoud M, de Gennes P-G. *J Phys (Paris)* 1977;38:85.
- [14] Teraoka I. *Polymer solutions. An introduction to physical properties*. New York: A John Wiley & Sons, Inc. Publication; 2002.
- [15] Meirovitch H. *Phys Rev A* 1985;32:3709.
- [16] Schmidt KE. *Phys Rev Lett* 1983;51:2175.
- [17] Sykes MF, Guttman AJ, Watts MG, Roberts PD. *J Phys A Gen Phys* 1972;5:653.
- [18] Wang Z, Luo M, Xu J. *Eur Polym J* 1999;35:973.
- [19] Le Guillon JC, Zinn-Justin J. *Phys Rev B* 1980;21:3976.
- [20] Cifra P, Romanov A. *Macromol Chem* 1986;187:2289.
- [21] Meirovitch H. *Macromolecules* 1983;16:249.
- [22] Meirovitch H. *Macromolecules* 1985;18:563.
- [23] Cheluvuraja S, Meirovitch H. *J Chem Phys* 2006;125:024905.
- [24] Zhao D, Huang Y, He Z, Qian R. *J Chem Phys* 1996;104:1672.
- [25] Wu D, Du P, Kang J. *Sci China Ser B* 1997;40:1.
- [26] Nowicki W. *Macromolecules* 2002;35:1424.
- [27] Dimitrov DI, Milchev A, Binder K. *J Chem Phys* 2006;125:034905.
- [28] Lipowsky R. *Europhys Lett* 1995;30:197.

- [29] Binder R. In: Domb C, Lebowitz J, editors. Phase transitions and critical phenomena, vol. 8. New York: Academic Press; 1983.
- [30] Whittington SG. *J Chem Phys* 1975;63(2):779.
- [31] Slutsky M, Zandi R, Kantor Y, Kardar M. *Phys Rev Lett* 2005;94:198303.
- [32] Cardy JL, Redner S. *J Phys A Gen Phys* 1984;17:L933.
- [33] Guttman AJ, Torrie GM. *J Phys A Gen Phys* 1984;17:3539.
- [34] De'Bell K, Lookman T. *Rev Mod Phys* 1993;65:87.
- [35] Barber MN, Guttman AJ, Midlemis KM, Torrie M, Whittington SG. *J Phys A Gen Phys* 1978;11:1833.
- [36] Ishinabe T. *J Chem Phys* 1985;83:423.
- [37] van Vliet JH, Luyten MC, ten Brinke G. *Macromolecules* 1992;25:3802.
- [38] van Giessen AE, Szleifer I. *J Chem Phys* 1995;102:9069.
- [39] Cacciuto A, Luijten E. *Nano Lett* 2006;6(5):901.
- [40] Romiszowski P, Sikorski A. *Biopolymers* 2000;54:262.
- [41] Sikorski A, Romiszowski P. *Biopolymers* 2003;69:391.
- [42] Sikorski A, Romiszowski P. *J Chem Inf Comput Sci* 2004;44:387.
- [43] Sikorski A, Romiszowski P. *J Mol Model* 2005;11:379.
- [44] Gan HH, Tropsha A, Schlick T. *J Chem Phys* 2000;113:5511.
- [45] Frenkel D. Introduction to Monte Carlo methods. In: Attig N, Binder K, Grubmüller H, Kremer K, editors. Computational soft matter: from synthetic polymers to proteins, lecture notes, vol. 23. Jülich; 2004. p. 29–60.
- [46] Sokal AD. In: Binder K, editor. Monte Carlo and molecular dynamics simulations in polymer science. New York: Oxford University Press; 1995.
- [47] Binder K. *Rep Prog Phys* 1997;60:487.
- [48] Skolnick J, Koliński A. *Adv Chem Phys* 1990;78:223.
- [49] Öttinger HC. *Macromolecules* 1985;18:9.
- [50] Madsen K, Nielsen HB, Tingleff O. Methods for non-linear least squares problems. In: Informatics and mathematical modelling. 2nd ed. Technical University of Denmark; 2004.
- [51] Watts MG. *J Phys A Gen Phys* 1975;8:61.
- [52] Sakaue T, Raphaël E. *Macromolecules* 2006;39:2621.
- [53] Daoud M, Jannik GJ. *J Phys (Paris)* 1976;37:973.
- [54] Surve M, Pryamitsyn V, Ganesan V. *Langmuir* 2006;22:969.
- [55] BonetAvalos J, Johner A, Díez-Orrite S. *Eur Phys J E* 2006;21:305.
- [56] Díez-Orrite S, Bonet Avalos J, Johner A, Joanny JF. *Macromol Symp* 2003;191:99.
- [57] Aubouy M, Raphaël E. *Macromolecules* 1998;31:4357.
- [58] Cassasa EF. *J Polym Sci* 1967;B5:773.
- [59] Hovorka S, Bayley H. *Biophys J* 2002;83:3202.
- [60] Viduna D, Limpuchová Z, Procházka K. *Macromolecules* 1997;30:7263.
- [61] Nowicki W, Nowicka G. *Can J Chem* 1997;75:1248.